Structure and stability of $Co_n(pyridine)_m^-$ clusters: Absence of metal inserted structures

B. Douglas Edmonds, A. K. Kandalam, and S. N. Khanna[a)]
Physics Department, Virginia Commonwealth University, Richmond, Virginia 23284-2000

X. Li, A. Grubisic, I. Khanna, and K. H. Bowen[b)]
Department of Chemistry, Johns Hopkins University, Baltimore, Maryland 21218

(Received 11 October 2005; accepted 13 December 2005; published online 21 February 2006)

A synergistic approach combining the experimental photoelectron spectroscopy and theoretical electronic structure studies is used to probe the geometrical structure and the spin magnetic moment of $Co_n(pyridine)_m^-$ clusters. It is predicted that the ground state of $Co(pyridine)^-$ is a structure where the Co atom is inserted in a CH bond. However, the insertion is marked by a barrier of 0.33 eV that is not overcome under the existing experimental conditions resulting in the formation of a structure where Co occupies a site above the pyridine plane. For $Co_2(pyridine)^-$, a ground-state structure is predicted in which the Co_2 diametric moiety is inserted in one of the CH bonds, but again because of a barrier, the structure which matches the photoelectron spectrum is a higher-energy isomer in which the Co_2 moiety is bonded directly to nitrogen on the pyridine ring. In all cases, the Co sites have finite magnetic moments suggesting that the complexes may provide ways of making cluster-based magnetic materials. © *2006 American Institute of Physics*. [DOI: 10.1063/1.2164455]

I. INTRODUCTION

Gas phase studies of organometallic complexes consisting of transition-metal clusters interacting with organic complexes have attracted considerable attention over the past few years. There are two principal reasons for the enhanced interest. First, such studies provide a convenient framework to study the interaction between the *d* electrons of the transition-metal atoms and π orbitals of the organic molecules without having to deal with the effect of solvents. An excellent example is the interaction between transition-metal atoms and benzene molecules. Secondly, supporting transition-metal atoms or clusters on molecular templates may provide novel ways of generating cluster-assembled materials. As an example, one may envision making magnetic materials where the transition-metal atoms/clusters retain their high magnetic moments attained in reduced sizes. Over the past few years, numerous such complexes have been reported.[1–7] For example, using laser vaporization techniques, Bowen and co-workers[6,7] and Kaya and co-workers[2,4] have generated $M_n(Bz)_m$ complexes containing 3*d* transition-metal atoms. Corresponding theoretical studies[8–12] revealed that the benzene molecules either sandwich the metal atoms forming multidecker sandwich structures or cage the metal atoms forming rice-ball structures. For example, the ground state of $Ni_2(Bz)_3$ is a structure where the two Ni atoms occupy sites between the three benzene molecules forming a rice-ball structure,[10] whereas the $V_n(Bz)_m$ complexes form multidecker sandwich structures.[12] Does the nature of the complexes change as one changes the metal atom and the organic molecule? Can these studies be extended to other systems?

In this paper, we report a synergistic effort in which anionic cobalt pyridine complexes are generated in beams and their photoelectron spectra recorded, while theoretical effort is directed toward understanding the geometrical structure, electronic properties, and the magnetic moments of the Co sites in these clusters. There are two basic issues that we wish to address. (1) What are the geometrical structures of the complexes? Specifically, is it possible for the Co atoms to be inserted in the CH bonds? (2) How are the magnetic moments of Co atoms modified in going from a free atom to the complexes? In particular, is it possible to form metal-organic complexes where the Co sites retain high magnetic moments? It is important to underscore here that atomic clusters are too small to directly probe the structure through microscopy. Similarly, for clusters containing less than five transition-metal atoms, the magnetic moments are too small to be accurately determined using the conventional Stern-Gerlach setup.[13] Here we demonstrate how a combination of the negative-ion photoelectron spectra and first-principles theory can overcome both of these obstacles and answer these questions.[14]

The present studies also bring out an intriguing feature frequented at small sizes, namely, that clusters of the same size and composition can exhibit different geometrical arrangements sometimes with different properties. Such a possibility arises due to the nature of the configuration space that is marked by distinct local minima protected by barriers. Depending on the conditions governing the formation, the clusters could be trapped in these minima. As an example, we had previously shown[15] that this trapping can lead to the observation of an otherwise unstable doubly ionized Be_3^{++}

[a)]Electronic mail: snkhanna@saturn.vcu.e
[b)]Electronic mail: kbowen@jhu.edu

cluster. We had demonstrated that while a simultaneous double ionization of a neutral Be_3 cluster leads to a unstable Be_3^{++} that fragments spontaneously, a sequential process where a singly ionized Be_3^+ is allowed to cool down to its equilibrium configuration before the removal of the second electron leads to a metastable Be_3^{++} that is protected from fragmentation by a barrier and hence can be observed. The present work presents another interesting scenario. We show that both $CoPy^-$ and Co_2Py^- feature ground-state structures where the Co atoms are inserted in the CH bonds. However, the insertion of the Co atom has a reaction barrier that is not overcome in the existing experimental conditions. Consequently, the observed structures are all non-ground-state structures. Interestingly, irrespective of the geometry, the Co sites in these anion complexes carry spin magnetic moment ranging from $1-3\ \mu_B$ per atom compared to a spin magnetic moment of $3\mu_B$ for the free atom and $1.7\mu_B$ in bulk. Even more interesting is the observation that the magnetic moments are the same for different structures thus indicating that the magnetic experiments cannot distinguish between the structures and that negative-ion photodetachment spectra that truly contain a fingerprint of the electronic structure are needed for the structural labeling.

II. METHODS

A. Experimental method

Negative-ion photoelectron (photodetachment) spectroscopy is conducted by crossing a mass-selected beam of anions with fixed frequency photon source and energy, analyzing the resultant photodetached electrons. This technique is governed by the energy-conserving relationship $h\nu$=EKE +EBE, where $h\nu$ is the photon energy, EKE is the measured electron kinetic energy, and EBE is the electron binding energy. The details of our apparatus have been described elsewhere.[16] Briefly, both mass spectra and photoelectron spectra were collected on an apparatus consisting of a laser vaporization source employing a Nd:YAG (yttrium aluminum garnet) laser, a linear time-of-flight mass spectrometer for mass analysis and selection, a second Nd:YAG laser used for photodetachment, and a magnetic bottle used for electron energy analysis.

Two ion sources were used to generate the clusters. One ion source consisted of an aluminum laser vaporization block with a rotating, translating cobalt rod (ESPI Company, purity 3N5) inside, a laser beam entrance port, and a gas expansion exit nozzle. A pulsed gas valve was mounted on the outside of this block. Typically, helium gas at 4 bars seeded with pyridine vapor was expanded into the source and synchronized with laser ablation pulses in order to generate the cobalt/pyridine cluster anions of interest. The cobalt rod was ablated with the second harmonic (532 nm) of a Nd:YAG laser.

The second source is similar to the first one except that pure helium gas was admitted through the pulsed valve described above, while helium seeded with pyridine was added ~2.5 cm downstream from the ablation laser through a second pulsed valve. In this source, pyridine did not interact with the ablation laser directly. Thus, cluster anions were formed by interactions between cobalt atomic and cluster anions and neutral pyridine molecules. This source is similar to that used by Klopcic *et al.*.[17] In both cases, the third (355 nm) harmonic of a second Nd:YAG laser was used to photodetach excess electrons from the cluster anions of interest. Photoelectron spectra were calibrated against the atomic lines of Cu^-.

B. Theoretical method

The theoretical studies were carried out using a linear combination of atomic-orbital–molecular-orbital approach. Here, the wave function of the cluster is expressed as a linear combination of the Gaussian functions centered at the atomic sites. The Kohn-Sham density-functional equations were then solved numerically on a mesh of points. The particular implementation we have used is called the Naval Research Laboratory Molecular Orbital Library (NRLMOL) and was developed by Pederson and Jackson[18] and Jackson and Pederson.[19] All the calculations were carried out at an all electron level, and the exchange-correlation contributions were included using a gradient-corrected density functional proposed by Perdew *et al.*[20] The basis set consisted of 7*s*, 5*p*, and 4*d* orbitals for Co; 5*s*, 4*p*, and 3*d* orbitals for N and C; and 4*s*, 3*p* and 1*d* orbitals for H. The basis sets were supplemented by 1*d* function for Co, N, and O, and by 1*p* and 1*d* orbitals for H. For other details, the reader is referred to earlier papers.[21]

In order to determine the ground-state geometries, two families of structures were tried: noninserted and inserted. In noninserted structures, the Co atom (atoms) was (were) initially located at various positions around the pyridine. Each of these structures was then optimized by moving atoms in the direction of forces and minimizing the energy until the forces dropped below a threshold. Different spin multiplicities were tried to determine the ground spin state. For the inserted structures, the preceding procedure was repeated by inserting the Co atom (atoms) in various bonds and repeating the optimization over the geometry and spin. In this case, we also examined the barriers for the insertion to examine the feasibility of the structures under the existing experimental conditions.

III. RESULTS

A. Experimental results

1. Mass spectra

We have generated cobalt pyridine cluster anions of the form $Co_nPy_m^-$. Figure 1(a) presents a typical mass spectrum taken with the single pulsed valve source, while Fig. 1(b) shows a mass spectrum recorded with the double pulsed valve source. Each $Co_nPy_m^-$ cluster exhibits a single dominant peak followed by a small shoulder resulting from the cumulative effect of the natural abundance of ^{13}C (1.1%). Both sources produced similar mass spectral patterns with negligible loss of hydrogen atoms from pyridine due to dissociative attachment. Generally, when $n=1$, m ranged from 1 to 3, when $n=2$, m ranged from 1 to 3 in the single valve source and from 1 to 4 in the double valved source, and when n

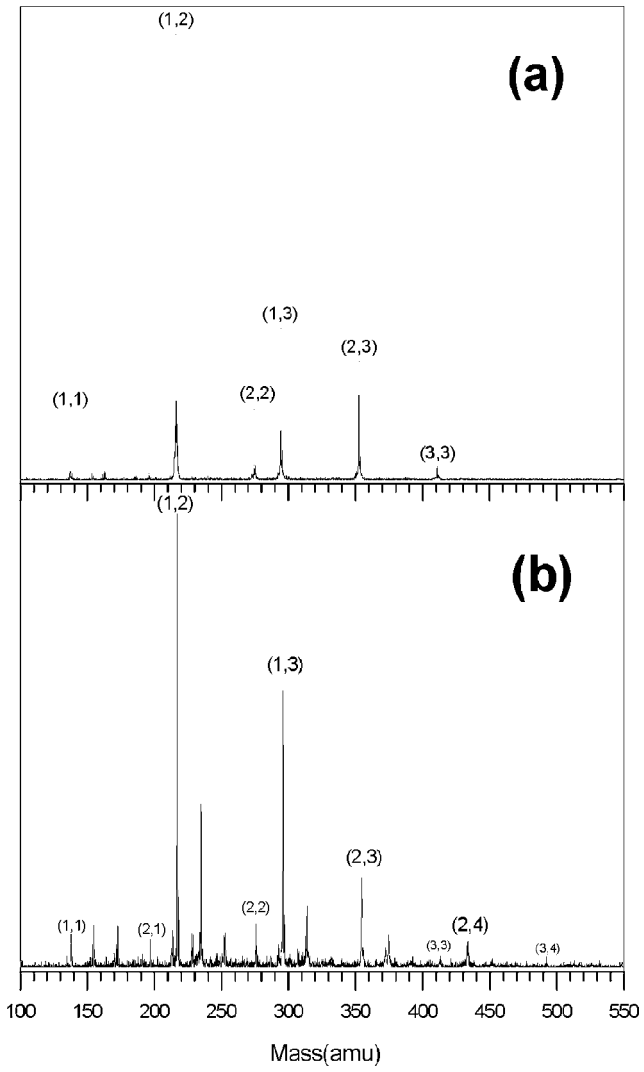

FIG. 1. The mass spectra of $Co_nPy_m^-$ clusters formed on (a) single pulsed valve source and (b) double pulsed valve source.

$=3$, $m=3$ in the former source as well as 3 and 4 in the latter source. However, there were also differences in the output of the two sources. The source with the single valve generated prominent peaks at (n,m) compositions of (1,1), (1,2), (2,2), (1,3), (2,3), and (3,3), with few impurities observed. The double valved ion source made higher intensities than the single valved source. As shown in Fig. 1(b), cluster compositions, (2,4) and (3,4) were observed in addition to the clusters that were formed with the other source, although more impurities were produced with this source.

2. Photoelectron spectra

We have recorded photoelectron spectra of all cobalt pyridine clusters observed in our mass spectra, except for (3,4) where the ion signal was too weak to collect a photoelectron spectrum. Additionally, we confirmed that the photoelectron spectrum of a particular ion was the same regardless of the source used.

The photoelectron spectra of $Co_1(Py)_1^-$ and $Co_2(Py)_1^-$ are compared in Fig. 2, while those of (1,2), (1,3), (2,2), (2,3), (2,4), and (3,3) are shown in Fig. 3. Each of these spectra depicts transitions from the electronic ground state of that

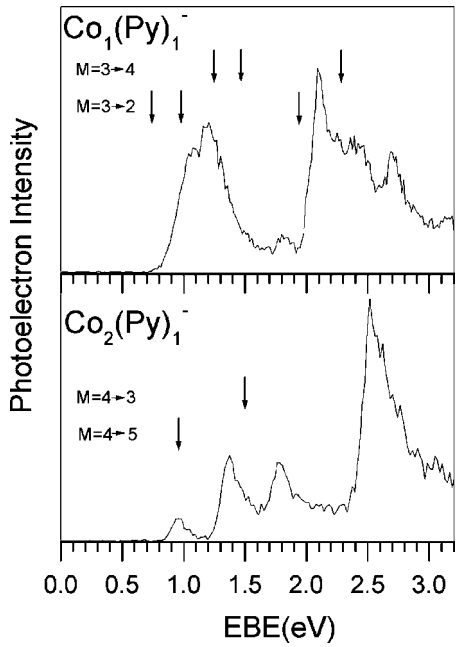

FIG. 2. Photoelectron spectra of $Co_1(Py)_1^-$ and $Co_2(Py)_1^-$. The vertical arrows indicate the calculated transition energies (see text for explanation). The spin multiplicities (M) of states involved in the transition are also marked.

particular cluster anion to the electronic ground state and energetically accessible excited states of its corresponding neutral cluster.

B. Theoretical results

As mentioned in the previous section, the photoelectron spectra involve a vertical transition from the anion of multiplicity M to the neutral species (at the geometry of anion) with multiplicity $M\pm1$. Comparison between the calculated transitions with experiment can therefore provide information on the geometry and the spin state of the anion. In this work, we have focused on $CoPy^-$ and Co_2Py^- to address some of the issues outlined in the Introduction. In Fig. 4 we have shown the ground-state and higher-energy geometries, the binding energy (BE) of the Co to pyridine, and the spin multiplicity of the $CoPy^-$ system. The binding energy was calculated using the equation

$$\mathrm{BE} = -E(\mathrm{CoPy}^-) + E(\mathrm{Co}^-) + E(\mathrm{Py}),$$

where $E(CoPy^-)$, $E(Co^-)$, and $E(Py)$ are the total energies of the $CoPy^-$, Co^-, and pyridine, respectively. Figure 5 shows the results of calculations for the Co_2Py^- system. In this case, the binding energy was calculated using the equation

$$\mathrm{BE} = -E(\mathrm{Co_2Py}^-) + E(\mathrm{Co_2^-}) + E(\mathrm{Py}).$$

In each case, vertical transitions from the anion to the neutral cluster with a spin multiplicity higher and lower than the anion were calculated. The transition energies along with their equilibrium geometries are provided in Figs. 4 and 5 for the $CoPy^-$ and the Co_2Py^- systems, respectively.

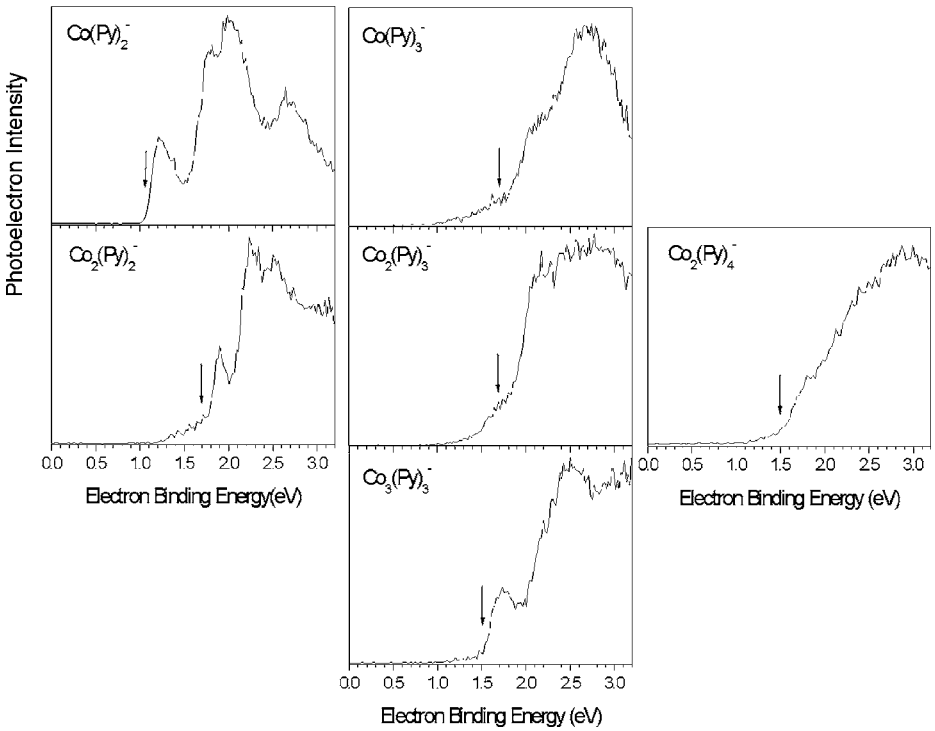

FIG. 3. Photoelectron spectra of the remaining six systems that were studied. The arrows indicate the assigned EA_a values.

IV. DISCUSSION

The ground-state geometry and other energetically degenerate structures of the $CoPy^-$ anion system are shown in Fig. 4. Note that the ground state of the cluster corresponds to a Co inserted in the CH bond opposite to the N atom. Inserting the Co in the CH bonds closer to the N site leads to a slight decrease in the binding energy of the system. However, the changes in energy are small, and the three structures can be considered energetically degenerate isomers. The inserted structures are followed by the noninserted structure that features a Co atom occupying a site above the pyridine and bonded to four C atoms. This noninserted structure is 0.46 eV less stable than the most stable inserted structure. It is interesting that all the anion structures have spin multiplicities of 3 and therefore spin magnetic moments of $2.0\mu_B$. An analysis of the spin charge density indicates that almost all of the spin moment is localized at the Co site. Their ground-state neutrals, on the other hand, have spin magnetic moments of $3\mu_B$ for the inserted cases and $1\mu_B$ for the on-face structure.

While the inserted structures are the most stable, their formation requires breaking of the CH bond and hence may be prevented by barriers. In order to further examine the feasibility of their formation, we calculated the reaction barrier for the formation of the most stable inserted structure. In these calculations, we calculated the total energy of the system for various values of the CH bond that would accommodate the Co atom. For each CH bond length, a Co atom was initially placed on top of the CH bond and the geometry was optimized maintaining the CH bond length. These calculations revealed a barrier of around 0.33 eV. Are the Co atoms able to overcome the barrier under the experimental conditions and form the inserted structures?

The experimental spectra (Fig. 2) are marked by a first broad peak with subpeaks around 1.1 and 1.2 eV. The broad peak starts around 0.7 eV and extends up to 1.5 eV. In addition, there are peaks at around 1.8, 2.1, 2.4, and 2.7 eV. None of the inserted structures have peaks below 1.90 eV. Consequently, we surmise that the Co atoms are not able to overcome the reaction barrier, under the experimental conditions that were utilized, to attain the inserted ground states. We would like to add that the peak positions at 1.8, 2.1, or 2.4 eV may be accounted for by some of the inserted structures suggesting the possibility that these structures may be present in the beam. If this were the case, one could confirm their presence by carrying out experiments under different conditions which should change the relative intensities of the peaks. We, however, did not detect any such changes in intensity excluding such a possibility.

To discern whether the noninserted structure could account for the photoelectron spectrum, we note that the calculated transition energy of 1.25 eV matches quite well with the observed peak at 1.2 eV. The calculated transition at 0.71 eV lies at the tail of the spectrum. The experimental subpeak at 1.1 eV and the higher-energy peaks at 1.8, 2.1, 2.4, and 2.7 eV require calculation of excited states. Here, the final state corresponds to the neutral cluster where the electronic levels below the highest occupied molecular orbital (HOMO) are unoccupied. The density-functional formalism used in this work is not well adapted for such excited-state calculations. However, one can carry out rough estimates by calculating the total energy of the neutral species where an electron in the HOMO was forced to occupy the next-higher one-electron level [the lowest unoccupied molecular orbital (LUMO)] leaving the initial HOMO unoccupied. Such rough estimates predict transition from $M=3$ anion to $M=2$ with excited states at 0.96 and 1.93 eV, while the transition from $M=3$ to $M=4$ has excited states at 1.46

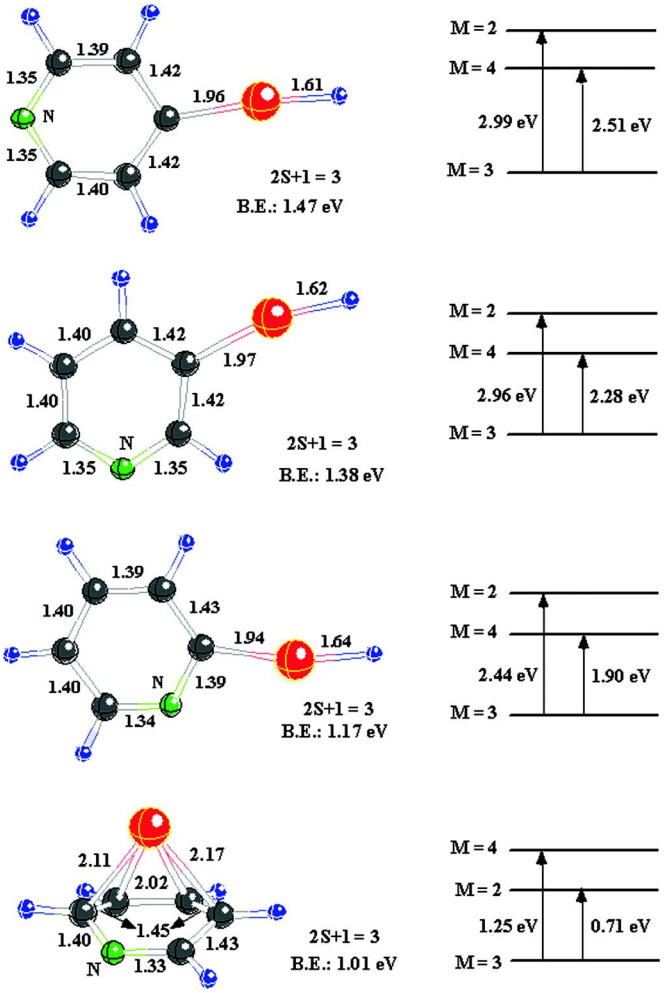

FIG. 4. The equilibrium geometries, binding energies, and the spin multiplicities of ground-state and higher-energy structures of $(Co_1Py)^-$ complex. Transition energies from the ground state of the anion to the corresponding neutral species with the same geometry as the anion are also shown.

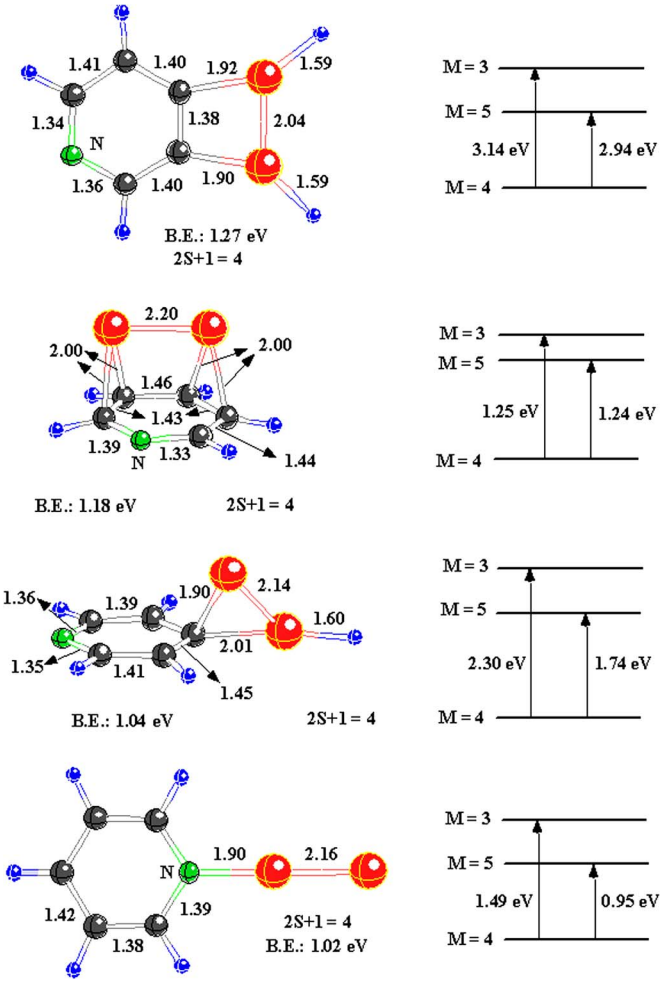

FIG. 5. The equilibrium geometries, binding energies, and the spin multiplicities of ground-state and higher-energy structures of $(Co_2Py)^-$ complex. Transition energies from the ground state of the anion to the corresponding neutral species with the same geometry as the anion are also shown.

and 2.28 eV. The combined transition energies of 0.96, 1.46, 1.93, and 2.28 have to be compared with corresponding observed values at 1.1, 1.8, 2.1, and 2.4 eV. In Fig. 2 we have marked the calculated transitions by vertical arrows and realizing that the calculated values are rough estimates, there does seem to be some correspondence.

In $(Co_2\text{-}Py)^-$ clusters, we tried various structures in which the two Co atoms occupied sites above the plane, bound to N atom, inserted in the CH bond, etc. Figure 5 shows the ground state and the energetically close structures for the Co_2Py^- cluster. As in the case of single Co, the ground state corresponds to the two Co atoms inserted in the CH bonds and bonded together to form a Co_2 molecule. Within 0.25 eV of this ground state are the structures where a Co_2 lies above the plane, a structure that requires breaking of one CH bond, and a structure where Co_2 binds to the N atom. To compare with the experimental spectra, we calculated the vertical transitions from the anion to the neutral species with a multiplicity one higher and one lower than the ground state. These transition energies are also shown in Fig. 5. The experimental spectrum shows transitions around 0.95 and 1.4 eV, respectively (see Fig. 2). The structure where a Co_2 is bound to the N site has transitions at 0.95 and 1.49 eV, and as shown by the vertical arrows in Fig. 2, these match the experimental transitions rather well. An analysis of the charge density on this structure reveals that most of the negative charge resides around the Co atom farthest from the nitrogen. This is interesting in view of the fact that the present spectra show striking similarity to the photoelectron spectrum of Co^- (Ref. 22) and not Co_2^-.[23] Further, the match of the three peaks in the spectra of Co^- and Co_2Py^- leads us to conclude that higher excited states of the single isomer are responsible for the observed peaks in the photoelectron spectrum of Co_2Py^-. Although, the observed peaks (1.8 and 2.6 eV) could also be accounted for by the structure with Co_2 moiety inserted into the single C–H bond (1.73 and 2.30 eV), as before, we believe that the barriers for the insertion into CH bond prevent the formation of the most stable structure in Fig. 5 under our experimental conditions.

Another interesting aspect is that the ground state of all the anion structures has a multiplicity of 4, implying a spin magnetic moment of $3.0\mu_B$. What is even more interesting is that the ground states of the neutrals all have spin multiplicities of 5, which correspond to spin magnetic moments of $4.0\mu_B$ or spin magnetic moments of $2.0\mu_B$ per Co atom. This is the same value as for a free cobalt atom but is higher than

the spin magnetic moment of $1.7\mu_B$ per Co atom in bulk Co. Thus, depending on the composition, charge state, and structure of a given cobalt/pyridine complex, its spin magnetic moment per Co atom can vary from 1 to $3\mu_B$.

While we have carried out calculations on only two of the cluster systems reported here, we have also measured the photoelectron spectra of several more compositions (see Fig. 3). One observes, for example, that the (1,2) cluster anion is very intense in the mass spectrum and that its photoelectron spectrum bears a strong resemblance to the previously reported spectrum of $Co(Bz)_2$ suggesting a similar geometry—possibly a sandwich structure.[6] Consistent with pyridine being a polar molecule (and benzene being nonpolar) its photoelectron peaks show a similar intensity pattern and a shift of ~0.5 eV toward higher EBE. Next, one notices that the species (2,2) and (3,3) have remarkably similar spectra with both exhibiting the same small peak at EBE ~1.8 eV and largely unstructured features above 2.3 eV. These two spectra also resemble the (2,2) and (3,3) spectra of the cobalt/benzene cluster system except for being shifted toward higher EBE by about 0.6 eV. Based on their similarity to the Co/benzene system and the observed mass spectral pattern, these are likely to be sandwich structures.

V. CONCLUSIONS

We have shown that while the ground-state configurations of $Co(Py)^-$ and $Co_2(Py)^-$ clusters involve Co atoms inserted in the CH bonds, the observed structures for $Co(Py)^-$ corresponds to Co adsorbed on top of the pyridine. A similar situation also occurs in Ni-Benzene complex where the ground state is an inserted structure but a large barrier prevents its formation.[24] This suggests that the observed structures of $Co_n(Py)_n^-$ and $Co_n(Py)_{n+1}^-$ may be sandwich structures. It may, however, be possible to overcome the barrier in experiments carried out at higher temperatures and hence it may be possible to design another class of complexes under different conditions. Irrespective of the structure, however, the Co atoms continue to carry large atomic moments making pyridine a possible substrate for preparing magnetic Co-based complexes.

ACKNOWLEDGMENTS

Both the experimental and the theoretical portions of this work were supported by the Division of Materials Science and Engineering, Basic Energy Sciences, U.S. Department of Energy. One of the authors (S.N.K.) was supported by Grant No. DE-FG02-96ER45579, while the other author (K.H.B.) was supported by Grant No. DE-FG02-95ER45538. Acknowledgment is also made to the Donors of The Petroleum Research Fund, administered by The American Chemical Society, for partial support of this research (Grant No. 28452-AC6).

[1] K. Hoshino, T. Kurikawa, H. Takeda, A. Nakajima, and K. Kaya, J. Phys. Chem. **99**, 3053 (1995).
[2] T. Yasuike, A. Nakajima, S. Yabushita, and K. Kaya, J. Phys. Chem. A **101**, 5360 (1997).
[3] P. Weis, P. R. Kemper, and M. T. Bowers, J. Phys. Chem. A **101**, 8207 (1997).
[4] T. Kurikawa, H. Takeda, M. Hirano, K. Judai, T. Arita, S. Nagao, A. Nakajima, and K. Kaya, Organometallics **18**, 1430 (1999).
[5] D. Van Heijnsbergen, G. von Helden, G. Meijer, G. Maitre, and M. A. Duncan, J. Am. Chem. Soc. **124**, 1562 (2002).
[6] M. Gerhards, O. C. Thomas, J. M. Nilles, W.-J. Zheng, and K. H. Bowen, J. Chem. Phys. **116**, 10247 (2002).
[7] W.-J. Zheng, J. M. Nilles, O. C. Thomas, and K. H. Bowen, Chem. Phys. Lett. **401**, 266 (2005).
[8] R. Pandey, B. K. Rao, P. Jena, and J. M. Newsam, Chem. Phys. Lett. **321**, 142 (2000).
[9] R. Pandey, B. K. Rao, P. Jena, and M. A. Blanco, J. Am. Chem. Soc. **123**, 3799 (2001).
[10] B. K. Rao and P. Jena, J. Chem. Phys. **116**, 1343 (2002); **117**, 5234 (2002).
[11] T. Yasuike and S. Yabushita, J. Phys. Chem. A **103**, 4533 (1999).
[12] A. K. Kandalam, B. K. Rao, P. Jena, and R. Pandey, J. Chem. Phys. **120**, 10414 (2004).
[13] I. M. L. Billas, A. Chatelain, and W. C. de Heer, Science **265**, 1682 (1994); S. N. Khanna and S. Linderoth, Phys. Rev. Lett. **67**, 742 (1991).
[14] S. N. Khanna and P. Jena, Chem. Phys. Lett. **336**, 467 (2001).
[15] S. N. Khanna, F. Reuse, and J. Buttet, Phys. Rev. Lett. **61**, 535 (1988).
[16] J. V. Coe, J. T. Snodgrass, C. B. Freidhoff, K. M. McHugh, and K. H. Bowen, J. Chem. Phys. **84**, 618 (1986).
[17] S. A. Klopcic, V. D. Moravec, and C. C. Jarrold, J. Chem. Phys. **110**, 8986 (1999).
[18] M. R. Pederson and K. A. Jackson, Phys. Rev. B **41**, 7453 (1990).
[19] K. A. Jackson and M. R. Pederson, Phys. Rev. B **42**, 3276 (1990).
[20] J. P. Perdew, K. Burke, and M. Ernzerhof, Phys. Rev. Lett. **77**, 3865 (1996).
[21] D. V. Porezag and M. R. Pederson, Phys. Rev. A **60**, 2840 (1999).
[22] R. R. Corderman, P. C. Engelking, and W. C. Lineberger, J. Chem. Phys. **70**, 4474 (1979).
[23] D. G. Leopold and W. C. Lineberger, J. Chem. Phys. **85**, 51 (1986).
[24] A. K. Kandalam, N. O. Jones, S. N. Khanna, and P. Jena, in *Clusters and Nano-Assemblies: Physical and Biological Systems*, edited by P. Jena, S. N. Khanna, and B. K. Rao (World Scientific, NJ, 2005), p. 341.